Food Eng Rev (2015) 7:64–81
DOI 10.1007/s12393-014-9098-3

REVIEW ARTICLE

Multiphysics Simulation of Innovative Food Processing Technologies

Kai Knoerzer · Roman Buckow · Francisco J. Trujillo · Pablo Juliano

Received: 16 June 2014 / Accepted: 6 October 2014 / Published online: 17 October 2014

Abstract Innovative food processing technologies, such as high-pressure (low and high temperature), pulsed electric field and ultrasound processing, can be applied to manufacture safe foods with better sensory and nutrition properties. These technologies can play an important role towards satisfying consumer demand for safe and innovative products, while reducing the carbon and water footprint, to promote more sustainable food manufacturing. The design, application and optimisation of suitable equipment and the selection of process conditions for these technologies require further knowledge development. Computational fluid dynamics has been established as a tool for characterising, improving and optimising traditional food processing technologies. Innovative technologies, however, provide additional complexity and challenges because of the interacting Multiphysics phenomena. This review will highlight a number of Multiphysics modelling case studies for the characterisation of various processing aspects and optimisation of selected innovative technologies. The underlying inactivation mechanisms, efficiencies and design limitations of these technologies are currently still under investigation and will be discussed.

Keywords Modelling · Simulation · High-pressure processing · Pulsed electric fields · Ultrasonics · Megasonics

K. Knoerzer (✉) · R. Buckow · P. Juliano
CSIRO Food and Nutrition Flagship, Melbourne, VIC, Australia
e-mail: kai.knoerzer@csiro.au

F. J. Trujillo
School of Chemical Engineering, University of New South Wales, Sydney, NSW, Australia

Introduction

The food industry is an increasingly dynamic arena with consumers being more aware of what they eat and, more importantly, what they want to eat. Important food quality attributes such as taste, texture, appearance and nutritional content are strongly dependent on the way foods are processed.

In recent years, a number of new and innovative food processing technologies, also referred to as "emerging" or "novel" technologies, have been proposed, investigated, developed and to some extent implemented with the aim to improve or replace conventional processing technologies. These technologies take advantage of physical phenomena other than heat, such as high hydrostatic pressure, dynamic sound pressure waves, or electric and electromagnetic fields, and provide the opportunity for the development of new food products or established food products with better acceptability and nutritional properties through gentle processing. Furthermore, these innovative technologies can potentially, through process intensification, lead to reduced energy and water consumption and, therefore, can play an important role towards economic and environmental sustainability of food processing and global food security by, for example, extending the shelf life of food products or expanding the shelf stable product spectrum [29].

In addition to the underlying thermo- and fluid-dynamic principles of conventional processing, these innovative technologies incorporate additional Multiphysics dimensions, for example, pressure waves and electric and electromagnetic fields, among others. To date, they still lack an adequate, complete understanding of the underlying physical principles and their interactions with the treated product [1]. The development and optimisation of suitable equipment to provide the

required process uniformity to achieve quality homogeneity among products remains a challenge. By improving the equipment design, processing parameters can be optimised to maximise product quality retention and increasing product acceptability.

Computational fluid dynamics (CFD) is an established tool for characterising, improving and optimising traditional food processing technologies; the partial differential equations solved are the ones describing the conservation of mass, momentum and energy (i.e. continuity, Navier–Stokes and Fourier equations). Innovative technologies, however, provide additional complexity and challenges for modellers because of the concurrent interacting Multiphysics phenomena; further, partial differential equations need to be solved simultaneously, such as the Maxwell and the constitutive equations for problems involving electromagnetics (e.g. microwave and radiofrequency processing), the charge conservation (e.g. pulsed electric field processing), and the wave equations (e.g. Helmholtz wave equations) for ultrasonic and megasonic processing [29]. These equation systems can increase in complexity when not only process variables, but also process targets or outcomes such as microbial/enzyme inactivation or food matrix modification are to be predicted. In such cases, the numerical problem is coupled to (differential) equations describing the dynamics of such phenomena, e.g. biological or chemical reactions and the development of (acoustic) forces leading to transport of concentrated species, among others [29].

Simulating Innovative Food Processing Technologies

As described extensively by various experts in the respective technologies in Knoerzer et al. [29], a common problem of innovative food processing technologies is the non-uniformity of the treatment, which can be caused by gradients of process variables such as temperature, electric field strength or sound pressure fields in the processing chambers. A non-uniform distribution of a certain process variable leads to non-uniformities in the resulting outcomes of the process (e.g. microbial inactivation or quality parameters).

While a trial-and-error approach is always an option to improve equipment and process design, it is the least preferred way, as it is very cost intensive, labour intensive, and time intensive and a good performance may be missed, as not all possibilities can be tested. On the other hand, numerical modelling using CFD can be used exactly for this purpose at reduced costs and time of experimentation. This way, advantages and disadvantages of the respective technology can be identified and either utilised or minimised.

Numerical modelling studies have been reported across the range of innovative technologies, such as microwave and radiofrequency, ultraviolet light, high-pressure, pulsed electric field, and ultrasonic processing. This review will focus on the latest advances in modelling high-pressure, pulsed electric field, and ultrasonic processing.

High-Pressure Processing

High-pressure processing (HPP) enables food preservation without using heat. HPP usually involves subjecting food to hydrostatic pressures of up to 700 MPa for a few minutes. This treatment inactivates vegetative microorganisms and some enzymes at room temperature, while valuable low-molecular constituents, such as vitamins, colours and flavours, remain largely unaffected. However, only when applied at elevated temperatures (e.g. >60 °C), high-pressure thermal processing (HPTP) can inactivate bacterial spores to obtain microbiologically safe and stable low-acid food products [46]. Accelerated and homogeneous heating and cooling of food occurs during HPTP due to the increase and decrease in temperature during the physical compression and decompression of the product. This facilitates uniform heating of all food packs and also reduces the need for excessively long heating times. HPTP products have improved food quality attributes, such as flavour, texture, nutrient content and colour, compared with thermal processing, due to reduced heat damage [45].

Over the last decade, a number of studies have reported on the utilisation of Multiphysics modelling for equipment and process characterisation in terms of process temperature and flow field distributions [11, 13, 22, 27, 28, 53], prediction of microbial spore and enzyme inactivation [17, 48] and equipment optimisation [24]. The work published on this topic before 2007 was summarised by Delgado et al. [8].

Process Characterisation

Knoerzer et al. [28] reported on the development and use of a numerical model to describe temperature and flow distribution in a 35-L pilot-scale high-pressure sterilisation system (Avure Technologies Inc., Kent, WA, USA) and evaluated the differences of the process variables for a number of different product carriers made of metal and insulating plastic material. The model was set up in COMSOL Multiphysics™ (COMSOL AB, Stockholm, Sweden) as a 2D axis-symmetric model, as the system only comprised of rotation-symmetric features, including gravitational forces due to the vertical arrangement. Figure 1 shows the temperature distributions in three investigated scenarios at the end of pressurisation to 600 MPa: namely,

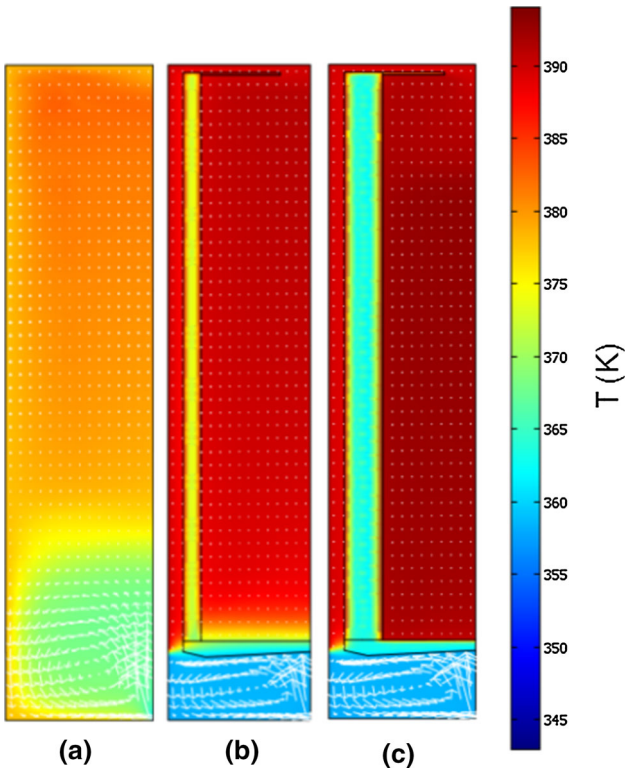

Fig. 1 Temperature distribution in an axis-symmetric section of the cylindrical high-pressure vessel; **a** no carrier in the vessel, **b** inclusion of cylindrical metal carrier and **c** inclusion of cylindrical PTFE carrier; at the end of pressurisation at 600 MPa (adapted from Knoerzer et al. [28]; for colour representation, the reader is referred to the online version of this article)

a cylindrical steel high-pressure vessel without carrier (Fig. 1a); one with a metal carrier (Fig. 1b); and one scenario where a carrier made from insulating polytetrafluoroethylene (PTFE) was placed into the vessel (Fig. 1c).

As shown in Fig. 1, the temperature distribution achieved in scenario (a) shows non-uniformities and relatively low temperatures compared to the scenarios where carriers are included, which avoid pronounced cooling down caused by the incoming pressurisation fluid. Temperatures in scenario (b) are more uniform, but still lower than in scenario (c). Furthermore, during pressure hold time, scenarios (a) and (b) exhibit pronounced heat losses, whereas the PTFE carrier in scenario (c) was able to retain the heat inside the carrier.

Knoerzer and Chapman [27] investigated the impact of process conditions and material properties on the accuracy of modelled predictions. They developed an axis-symmetric model approximating a Stansted 3.6 L Isolab HPTS system (Stansted Fluid Power Ltd, Stansted, UK) in COMSOL Multiphysics and studied the effect of utilising simplified pressure profiles (i.e. linear increase in pressure during pressurisation, constant pressure during pressure hold time and linear decrease in pressure during decompression) in the model versus pressure profiles measured in the system. Furthermore, they evaluated the impact of using simplified compression heating properties (e.g. those well known for water) versus experimentally determined compression heating properties for the actual compression fluid (water–glycol mixture), as determined by Knoerzer et al. [25], on the prediction accuracy. They found that inaccurate approximation of both input conditions for the pressure profiles and the material properties resulted in highly inaccurate predictions (Fig. 2) and highlighted the importance of attention to detail with respect to input data for CFD models of HPTP to ensure that models delivered accurate predictions.

Khurana and Karwe [22] described a 2D axis-symmetric model of an experimental pilot-scale (10 L) HPP system (Elmhurst Research Inc., Albany, NY, USA) in Fluent® (Fluent Inc., Lebanon, NH, USA). They reported, similar to Knoerzer et al. [28], that heat losses occur when the vessel walls are cooler than the temperature of compression fluid and product after compression. Possible improvements of thermal performance through the inclusion of insulated product baskets were not reported in their work.

As opposed to the 2D axis-symmetric approximations of high-pressure systems, Ghani and Farid [11] have developed a full 3D model in Phoenics 3.5 (Concentration, Heat and Momentum Ltd, London, UK) of a significantly smaller (approximately 330 mL), vertically oriented, labscale system (Foodlab S-FL-850-9-W, Stansted Fluid Power Ltd, Stansted, UK) capable of predicting flow and temperature patterns in liquid and solid food products (Fig. 3). The authors suggested that this study was the first to report on the effect of forced convective heat transfer on the temperature distribution in liquid foods undergoing high-pressure treatment caused by the pressure transmitting fluid entering the treatment cylinder, as well as the distribution of temperatures in liquid and solid food products at different time steps during high-pressure processing. However, as described in Delgado et al. [8], CFD studies of this kind, i.e. prediction of temperature and flow distributions during HPP at low temperatures (i.e. in the order of 10–50 °C), have been published as far back as 2000.

The trend in commercial application of high-pressure technology is towards using horizontal systems rather than vertical ones, due to easier loading and unloading of the product baskets [44]. However, most modelling studies available in the public domain report on models describing vertically oriented high-pressure systems. Very few, e.g. Grauwet et al. [13] and Smith et al. [53], evaluated models in horizontal vessel orientation. The model reported in Grauwet et al. [13] will be discussed in the next section, as

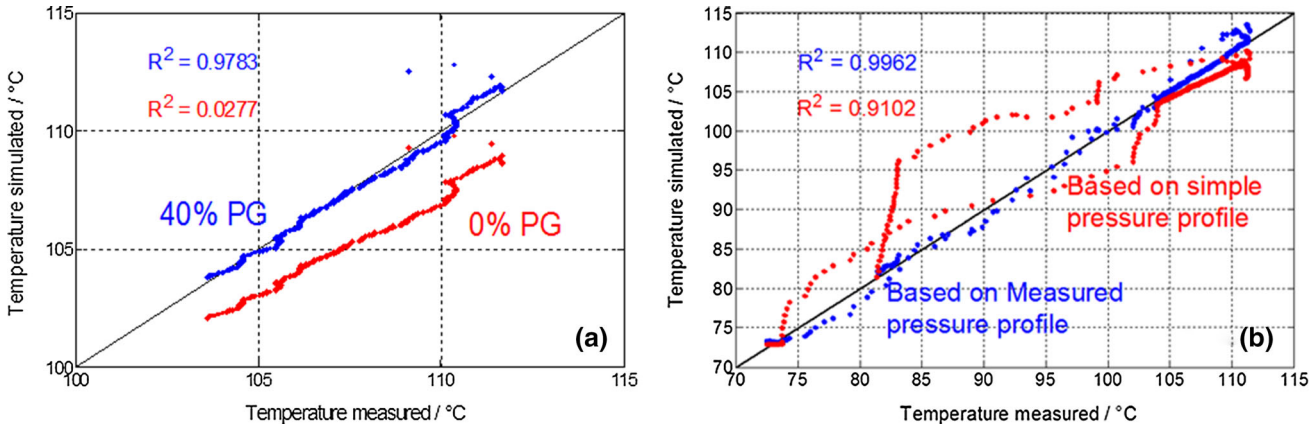

Fig. 2 **a** Parity plots of simulated versus measured temperature profiles, when using compression heating properties of water (*red*) and actual compression fluid (water–propylene–glycol (PG)) (*blue*); **b** parity plots of simulated versus measured temperature profiles, when using simplified pressure profile (*red*) and representative pressure profile from the HP system (*blue*) (adapted from Knoerzer and Chapman [27]; for colour representation, the reader is referred to the online version of this article) (Color figure online)

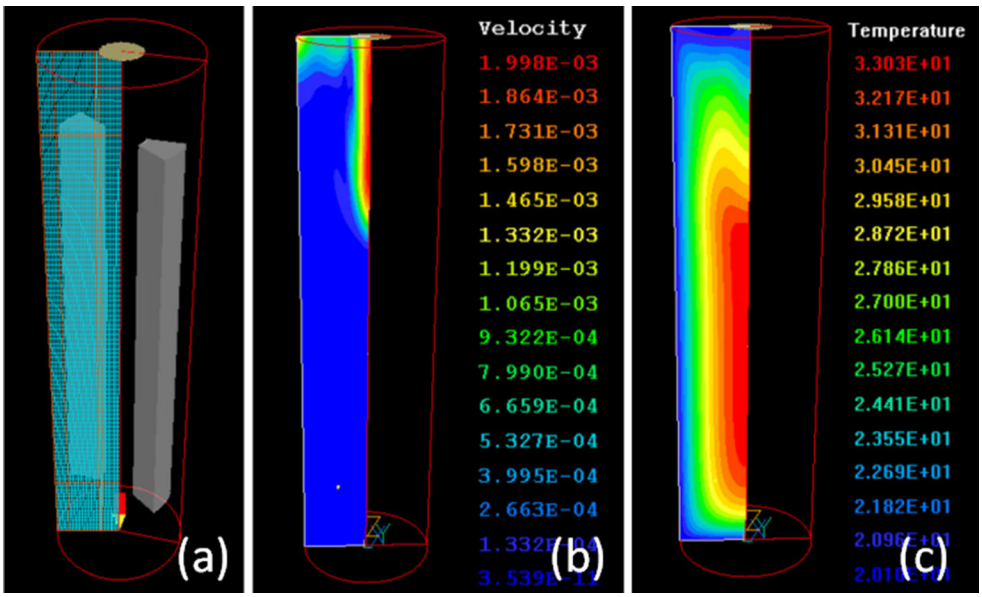

Fig. 3 **a** 3D computational grid of the modelled high-pressure system including the solid food pieces, **b** predicted velocity distribution after 24 s of compression and **c** predicted temperature distribution just before reaching target pressure (adapted from Ghani and Farid [11]; for colour representation, the reader is referred to the online version of this article)

it comprises coupling of the CFD model predictions to enzyme inactivation models.

The objective in the work reported by Smith et al. [53] was to evaluate the differences in thermal performance, i.e. temperature distribution, during HPTP when comparing the same high-pressure system in vertical and horizontal orientation. Given the fact that gravitational (buoyancy) forces are not rotation-symmetric in horizontal orientation, 3D models were developed in COMSOL Multiphysics for both orientations (Fig. 4a). Significant differences in temperature profiles were reported when comparing both orientations (Fig. 4b), and more temperature uniformity in the horizontal orientation (Fig. 5). While the first finding was expected, the latter finding is of particular relevance, as it confirms that horizontal HPTP vessels have, in addition to other benefits, the advantage of providing greater temperature uniformity.

Prediction of Bacterial Spore and Enzyme Inactivation

The model developed by Knoerzer et al. [28] showed that only an insulated carrier provides process conditions feasible for sufficient and relatively uniform product sterilisation. Juliano et al. [17] applied more detailed CFD

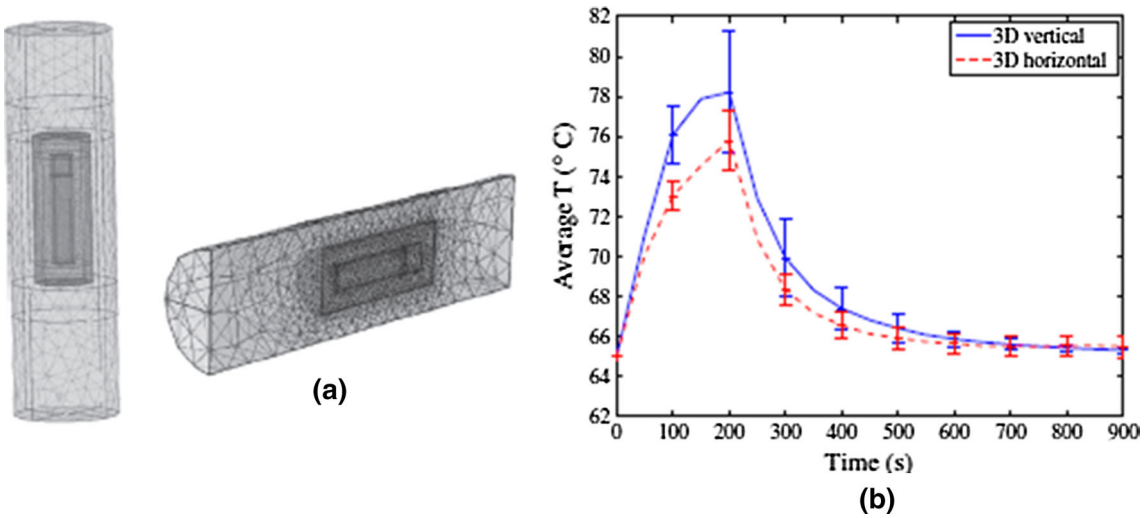

Fig. 4 **a** Computational approximation of the high-pressure system in vertical (*left*) and horizontal orientation (*right*); **b** differences in temperature profile averaged over a matrix of the vessel content at a resolution of 1 mm^3 (adapted from Smith et al. [53])

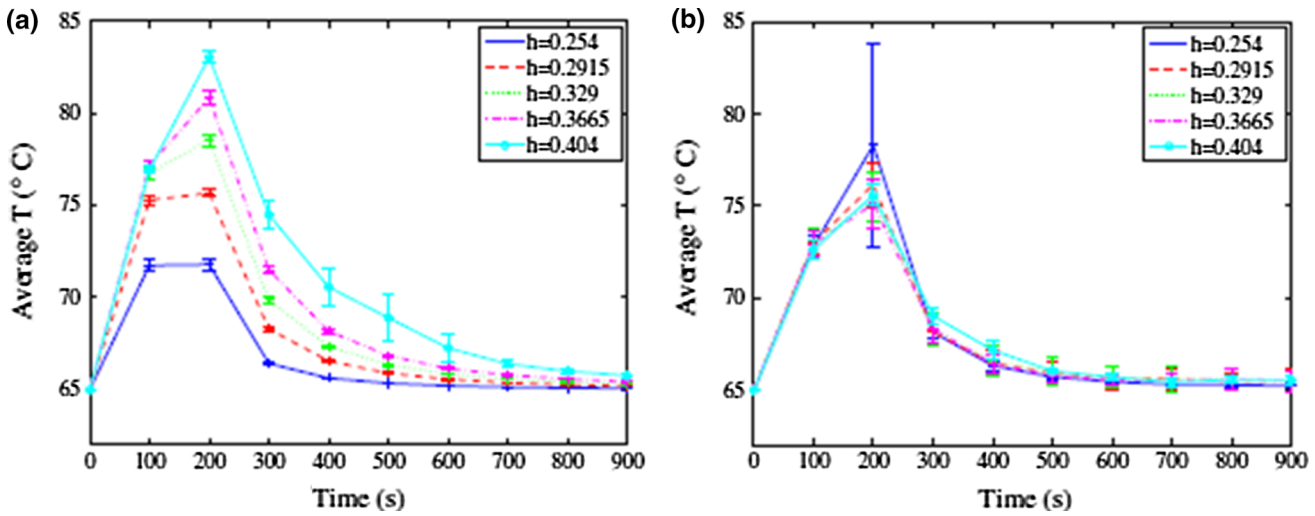

Fig. 5 Differences of temperature profiles averaged over five equidistantly spaced radial slices in the vertically (**a**) and horizontally (**b**) oriented high-pressure system (adapted from Smith et al. [53])

models of the high-pressure system with food packs filled with water (Fig. 6a), describing the process variables (i.e. pressure, temperature and flow) and evaluated the differences in the extent of predicted inactivation of *C. botulinum* spores in food packages. In the first step, the CFD models were able to show better heat retention inside the food packs than in the surrounding liquid during pressure hold time (Fig. 6b, c).

The predicted transient temperature distributions were then coupled to selected predictive spore inactivation models, namely the commonly known log-linear model, an nth order model and a Weibull distribution model. The different inactivation models predicted very different levels of spore inactivation for the same process. For example, the log-linear model predicted inactivation of *C. botulinum* spores in the food packs in the order of 16 $\log_{10}$ after 3 min processing at 600 MPa and 121 °C (Fig. 6d), whereas the Weibull model indicated spore inactivation of only 9 $\log_{10}$ for the same process (Fig. 6e).

Rauh et al. [48] investigated the impact of different thermal boundary and initial conditions on the uniformity of enzyme inactivation during HPP with a maximum pressure of 700 MPa. They developed a 3D model in Ansys ICEM CFD and CFX (Ansys Inc., Canonsburg, PA, USA), extended by self-developed codes in FORTRAN of a vertically oriented HP vessel and predicted fluid streaming profiles, temperature and enzyme activity fields in the treatment chamber. Depending on the parameter

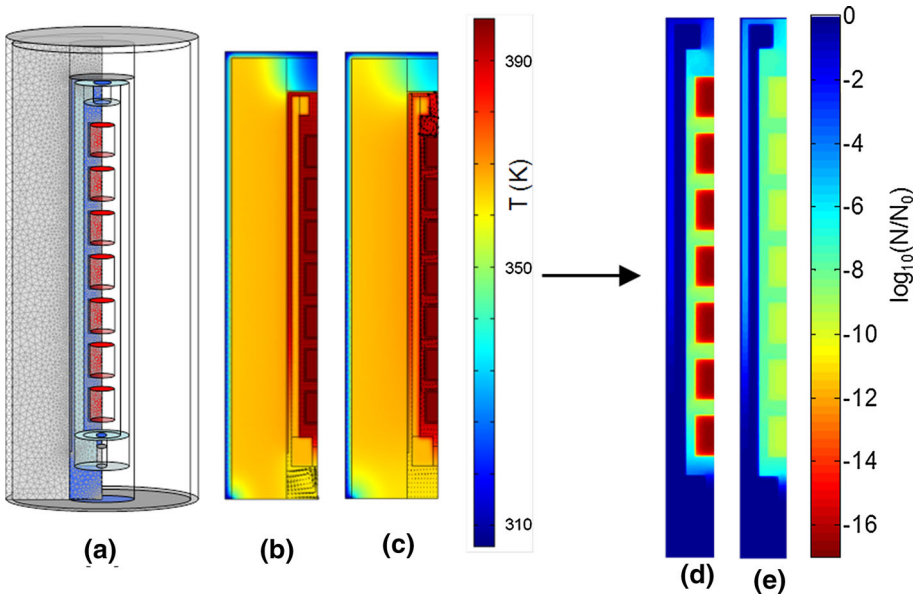

Fig. 6 **a** Model geometry, **b** predicted temperature distributions at the end of pressurisation and **c** pressure hold time; **d** indication of inactivation of *C. botulinum* spores as predicted by a log-linear model and **e** a Weibull distribution model (adapted from Juliano et al. [17]; for colour representation, the reader is referred to the online version of this article)

settings, process non-uniformities were seen in residual activities of a β-glucanase, α-amylase, lipoxygenase, polyphenoloxidase enzyme (each possessing a specific pressure sensitivity and temperature sensitivity) during the process, caused by temperature non-uniformities; however, they also reported that the viscosity of the pressurised material contributes to the occurrence and extent of temperature non-uniformities during the process. Therefore, uniform temperature distributions do not necessarily lead to more effective processing results. This work was extended by Grauwet et al. [13], where the previously described model was modified to also allow for predictions in horizontal orientation and for different vessel volumes. Based on the models and temperature indicators, temperature distribution and subsequently enzyme inactivation are strongly dependent on vessel dimension, orientation, boundary/process conditions, pressure generating system (piston system versus external high-pressure pump), pressure medium and treated product. The authors also report a number of different implementation strategies to improve temperature uniformity and that many of these insights have been gained through modelling. These strategies include, for example, selecting components in the vessel content with similar compression heating properties (including packaging materials and food products), equilibration of vessel contents to the same initial temperature, using direct compression (piston system) rather than indirect compression through injection of water/compression fluid, and selecting (insulating) product carriers with similar compression heating properties as those of the vessel content and compression fluid (as also reported by Knoerzer et al. [26]). The list goes on, but in a commercial environment, it is our opinion that only indirect compression systems with appropriately insulated product carriers undergoing compression heating enabling utilisation of non-heated, horizontally oriented high-pressure systems will lead to commercial success of HPTP.

Equipment Optimisation

Knoerzer et al. [24] used a modified version of the model described by Juliano et al. [17] to optimise the wall thickness of the insulating carrier while increasing product load capacity. The carrier supplied by the manufacturer was designed with a wall thickness such that sufficient heat retention was ensured during processing. The authors derived a dimensionless parameter, referred to as integrated temperature distributor (ITD) value (Eq. 1) to evaluate temperature uniformity, and the temperature magnitude expressed relative to a target temperature and heat retention during processing.

$$\mathrm{ITD} = \frac{\int_{r_{\min}}^{r_{\max}} \int_{z_{\min}}^{z_{\max}} 10^{\frac{\int_0^t T(t)\mathrm{d}t}{t} - T_{\mathrm{target}}} \mathrm{d}r\mathrm{d}z}{(r_{\max} - r_{\min}) \cdot (z_{\max} - z_{\min})} \quad (1)$$

where $r_{\min}$, $r_{\max}$, $z_{\min}$ and $z_{\max}$ (in m) cover the region of interest (the carrier volume), t (in s) is the process time of interest (in this case, the pressure holding time where most of the heat loss is expected), T_{target} (in °C) is the targeted holding temperature of the process under pressure, $T(t)$ is the transient temperature profile, and z_T (in °C) is the thermal sensitivity.

An iterative strategy was applied, which consisted of a model that automatically changed the carrier wall thickness

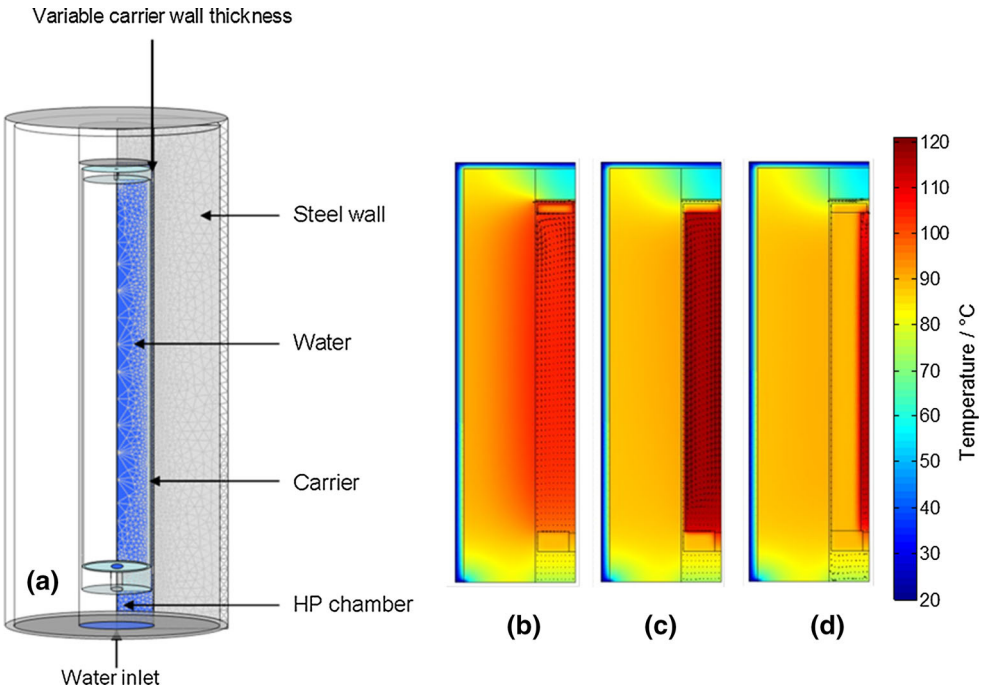

Fig. 7 Depiction of the model geometry (**a**) and the predicted temperature distributions using a carrier with a wall thickness of 0 (**b**), 5 (**c**) and 70 mm (**d**) (adapted from Knoerzer et al. [24]; for colour representation, the reader is referred to the online version of this article)

over a range of 0–70 mm and evaluated the temperature performances and load capacities for the respective scenarios. Figure 7 shows the modified model geometry with variable carrier wall thickness and the predicted temperature distributions at the end of pressure hold time for a wall thickness of 0, 5 and 70 mm.

The study showed that the wall thickness could be reduced from 28 mm to approximately 4 mm without compromising temperature retention, leading to an increase in carrier load capacity of more than 100 %.

Pulsed Electric Field Processing

Pulsed electric field (PEF) processing is a technology that can be applied for food preservation at room or sub-pasteurisation temperatures and, therefore, can improve the quality attributes of foods compared to conventional thermal processing. It involves the application of very short, high voltage pulses to a food which is placed between or pumped through two electrodes. PEF disturbs and perforates biological cell membranes leading to cell death. Microbial inactivation efficiency of PEF is dependent on cell characteristics (i.e. structure and size) and extrinsic factors such as product pH, water activity, soluble solids and electrical conductivity. PEF often requires application of pulses with a duration of microseconds and field strength between 20–50 kV per centimetre [4]. This technology can also be used to enhance extraction processes or soften of fruit and vegetable tissue, for example for improving cutting performance and reducing cutting losses. Being a continuous process, high throughputs are possible.

Numerical modelling of PEF processing has been used for process characterisation of batch PEF systems with respect to temperature and pH gradients [42, 51] and electric field, temperature and flow distributions in continuous PEF systems [3, 5, 10]. Recently, numerical simulations of the PEF processes have been coupled with predictive inactivation models for microorganisms and enzymes [6, 30]. This approach can significantly contribute to the development and design of effective PEF equipment and processes [31].

Early simulation studies of PEF processing described distributions of temperature and electric field strength in the treatment zones of laboratory-scale, co-linear treatment chambers and reported local temperature hot spots due to limited flow velocity and mixing of the liquid [9, 39]. These process parameters are only detectable using mathematical simulations as measurement in the confined space (typically only a few microlitres) of the treatment chamber is not possible without major interference of the flow and electric fields by measuring devices. Fiala et al. [9] and Lindgren et al. [39] also applied numerical methods to evaluate different geometry of electrodes and insulators in a co-linear PEF chambers and their effect on distributions of the electrical field strength. Both studies concluded that the shape and dimensions of electrodes and insulators highly affected distributions of the electric field strength and electrodes and insulators should be positioned in a 90° angle to each other to avoid major peaks of the electrical field strengths in this area.

Gerlach et al. [10] reviewed the literature on numerical simulations of PEF before 2007 and concluded that the

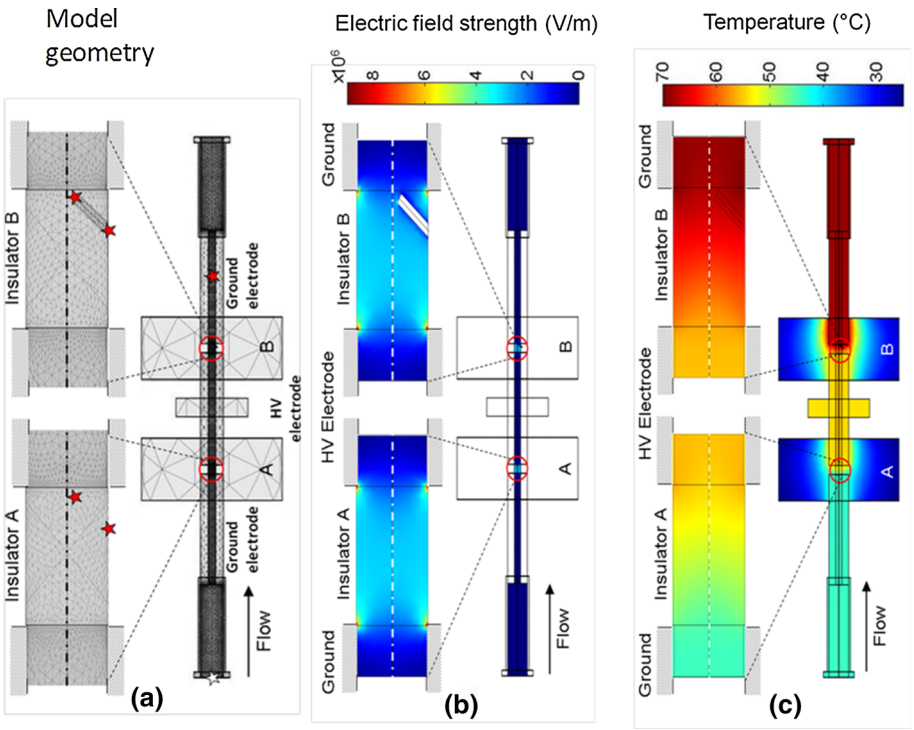

Fig. 8 Representation of the pilot-scale PEF treatment chamber including magnification of the treatment zones (**a**), electric field strength (**b**) and temperature (**c**) distribution in a salt solution at specific processing conditions (adapted from Buckow et al. [5]; for colour representation, the reader is referred to the online version of this article)

numerical approach should be used to enhance treatment uniformity in PEF treatment chambers by systematic optimisation algorithms that automatically adjust the insulator geometry until a uniformity maximum of the electric field is found. However, the review also highlighted the need to couple simulations of the fluid flow, electric field and thermal convection and conduction to obtain more accurate results.

Jaeger et al. [14] used numerical simulations to improve PEF treatment uniformity and, thus, the effectiveness of the treatment to inactivate microorganisms and enzymes. Metal and polypropylene grids were inserted into the treatment chamber to improve the field strength distribution, mixing effects and, as a result, temperature uniformity during the treatment. The authors demonstrated that the suggested chamber modification resulted in more effective inactivation of microorganisms while (largely thermal) inactivation of enzyme systems can be avoided. Similarly, the authors showed in other studies that the shape (rectangular vs convex) of the insulator in a co-linear PEF treatment chamber affects the effectiveness of the treatment to inactivate microorganisms and retention of enzyme activity [41, 43]. A convex shaped insulator yielded slightly higher inactivation of *Escherichia coli* in Ringer solution than an insulator with a rectangular shape under similar process conditions. Furthermore, cooling of the electrodes limited the temperature rise of the fluid during PEF processing at low flow rates (i.e. 4 L/h) resulting in larger retention of enzymes.

Kang et al. [21] compared the process uniformity of a co-linear and a co-axial PEF treatment chamber. Numerical simulations indicated that a co-axial arrangement of electrodes improves the overall uniformity of the electric field and results in a more uniform temperature increase than the co-linear arrangement. As a result, microbial reduction in water melon juice was larger in the co-axial equipment than in the co-linear equipment under similar PEF process conditions.

Buckow et al. [5] developed a 3D model for a pilot-scale PEF system (Diversified Technologies Inc., Bedford, MA, USA) to predict electric field strength, flow and temperature distributions (Fig. 8) and extensively validated the model predictions through temperature measurements within the constrained space of the treatment chamber's active zone. The authors were able to utilise this model to characterise and evaluate the performance of the system as supplied by the manufacturer with respect to electric field strength, temperature and flow distribution.

Buckow et al. [3] applied this model further to derive simplified equations to estimate accurate electric field strengths and specific energy inputs from treatment variables such as voltage, pulse frequency and duration among others. The effects of changing treatment chamber geometry and configuration on these process variables were also evaluated. A common approach for estimating the electric field strength is relating the applied voltage to the electrode gap. While this will give accurate predictions for parallel plate systems, it was found that for configurations used in

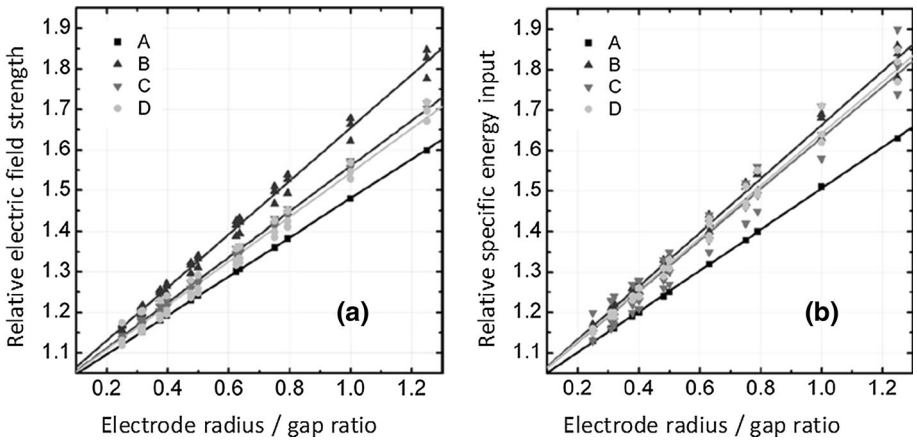

Fig. 9 Correlation of **a** the relative electric field strength and **b** the relative specific energy input with the ratio of electrode radius to gap for "no inset" (*A*), "rectangular inset" (*B*), "chamfer edge" (*C*) and "elliptical inset" (*D*) chamber configurations (adapted from Buckow et al. [3])

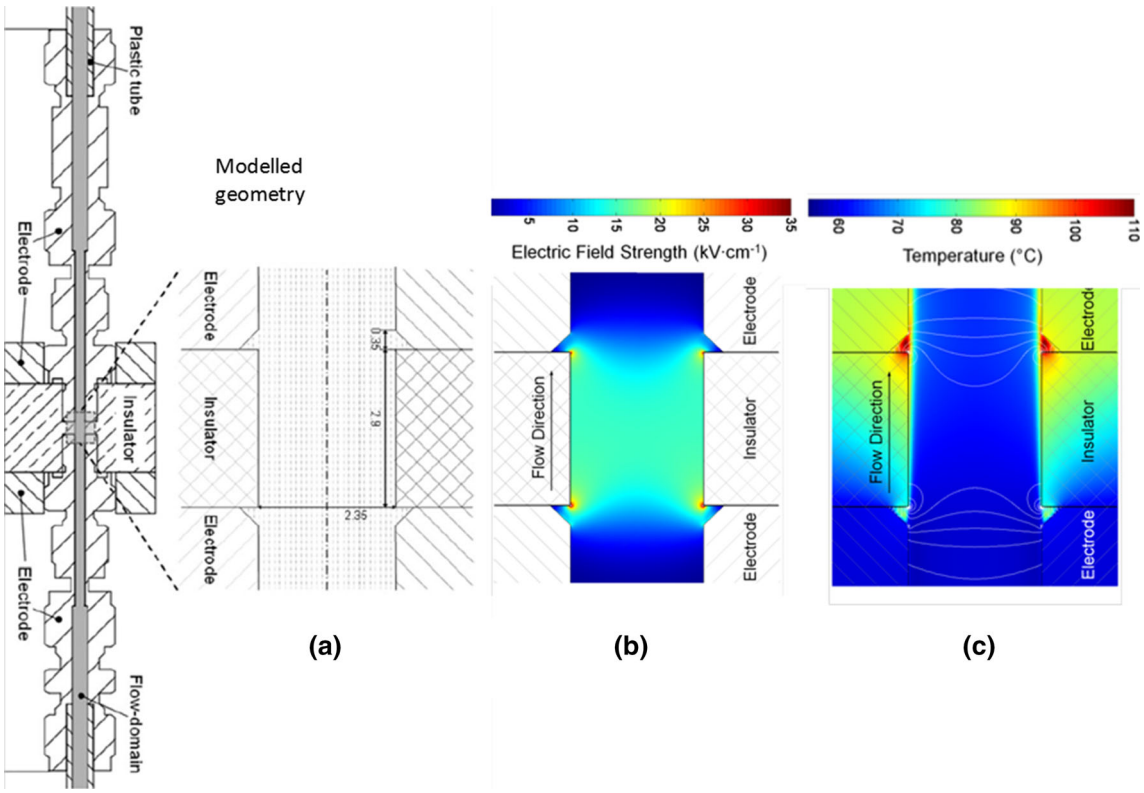

Fig. 10 **a** Representation of the modelled geometry of the laboratory-scale PEF system, **b** predicted electric field distribution and **c** predicted temperature distribution (**c**) at specific processing conditions (adapted from Buckow et al. [6]; for colour representation, the reader is referred to the online version of this article)

continuously operating systems, such as co-field or co-linear designs, this approach always over-predicts the actual electric fields. This is similar for specific energy input, commonly estimated by multiplying voltage, current, pulse width, pulse repetition rate and mass flow. Figure 9 shows (a) the correlation of relative electric field strength (i.e. actual electric field strength divided by estimated electric field strength for parallel plate configuration) and (b) the correlation of the relative specific energy input (i.e. the actual specific energy input divided by estimated specific energy input for parallel plate configuration) with the ratio of electrode radius and electrode gap for different chamber configurations. These configurations were as follows: "no inset" (where the insulator bore diameter is equal to the inner electrode diameter), "rectangular inset" (where the insulator bore diameter is smaller than the inner electrode radius), "chamfer edge inset" (which is identical to the rectangular inset with rounded edges of the insulator

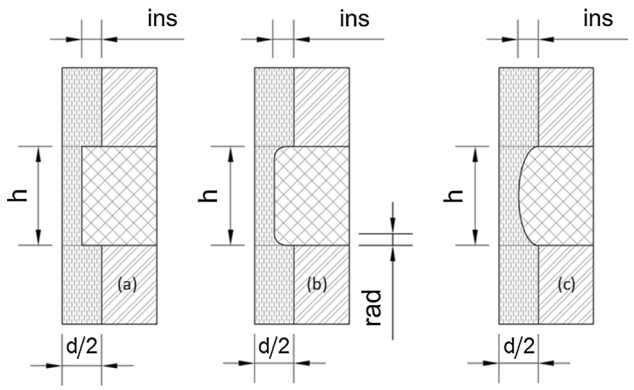

Fig. 11 Investigated chamber configurations indicating the geometrical parameters varied in the model; **a** rectangular inset, **b** rectangular chamfered edge inset and **c** elliptical inset scenario (from Knoerzer et al. [31])

bore) and "elliptical inset" (where the insulator bore has an inward concave shape), see also Fig. 11.

Buckow et al. [6] then developed and validated a model for a laboratory-scale PEF system (Fig. 10a) and evaluated the effect of the electric field on lactoperoxidase (LPO) inactivation (an indicator for thermal pasteurisation of milk) by coupling the predicted temperature distributions (e.g. Figure 10c) to thermal inactivation kinetics of LPO.

The study indicated that the major effect of PEF processing on LPO inactivation comes from the elevated process temperatures as the predictions (thermal-only inactivation) were close to the measured inactivation (combined thermal and PEF) for a number of process conditions. However, they found that there was also some additional inactivation caused by the electric field of up to 12 % possibly caused by induced electrochemical reactions.

Knoerzer et al. [31] developed an iterative algorithm that was capable of automatically changing the treatment chamber configuration and dimensions in the Multiphysics models. The algorithm also identified, out of more than 100,000 scenarios, the treatment chamber design that showed the highest degree of electric field uniformity, together with sufficient throughput, lowest pressure drop, among other evaluation characteristics. The evaluation of the performance of the models was based on a parameter, referred to as dimensionless performance parameter (DPP), calculated by an equation derived by the authors, accounting for the treatment volume, pressure drop estimations, electric field magnitude related to that achievable in parallel plate systems, electric field uniformity and peaks of the electric field strength.

Three different chamber configurations (Fig. 11) were studied and for each of these, four different geometry parameters were varied: the internal diameter d of the electrodes ranging from 2 to 20 mm, the height h of the electrode gap ranging from 1 to 30 mm, a total inset *ins* (i.e. the internal diameter of the insulator) in a range of 0–90 % of the electrode diameter d, and for the "rectangular rounded edge inset" models also the chamfer radii *rad* ranging from 0 to 40 % of the diameter reduction *ins* (Fig. 11).

The algorithm first generated the models, then solved them, applied the performance evaluation by utilising the DPP equation and then identified the scenario which yielded the highest DPP value, which was found for configuration (b). The authors then set up a full 3D model of this configuration, built the new chamber and performed validation studies of the model for a salt solution and apple juice and for various process conditions. They found that the new design could be predicted well with respect to the temperatures generated in the treatment chamber.

Ultrasonics and Megasonics Processing

Ultrasound processing spans over a wide range of acoustic frequencies, starting as low as 18 kHz, up to several MHz. Applications are as diverse as the frequency spectrum is wide. At the lower frequency end (18 kHz to approximately 200 kHz, also referred to power ultrasonics), the effects are caused mainly by instable cavitation. Traditional applications such as emulsification, cleaning, and extraction [12], and more novel applications used for improved drying [2, 50] and beverage defoaming [49] in airborne ultrasound systems can be listed. When using higher frequencies (>400 kHz, also known as Megasonics), the effects can be either mechanical through standing pressure waves and microstreaming, and/or sonochemical (radical driven) or biochemical (stress response in living tissue). Novel high-frequency applications include the separation of particles in standing wave systems [18–20], and texture improvement of processed fruits and vegetables, through produced internal stress responses [7].

The few studies on numerical modelling of ultrasonics and megasonics relevant to food processing that can be found in the public domain include the utilisation of Multiphysics models for equipment characterisation with respect to acoustic pressure, temperature, flow, cavitation distribution and equipment optimisation [15, 16, 23, 52, 56] for low-frequency ultrasound and for predicting particle separation [54] and micromixing characteristics [47] for high-frequency ultrasound.

In spite of several potentially promising applications of low-frequency ultrasound, there have been problems in scaling up to industrial scale. This is due to the fact that acoustic pressure in sonoreactors is generally not uniformly distributed, resulting in sonochemically active and passive zones [34]. The major problem for scaling up strategies is

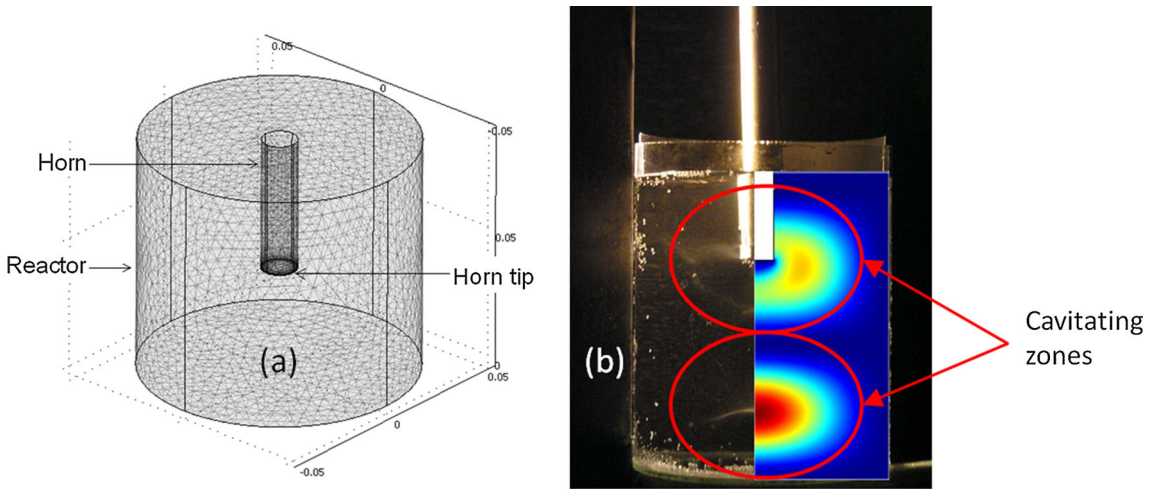

Fig. 12 **a** 3D model of the utilised ultrasound reactor; **b** qualitative validation of the model predictions by comparing the sound intensity distribution with photographs of the cavitation zones of the same set-up (adapted from Klima et al. [23]; for colour representation, the reader is referred to the online version of this article)

that cavitational activity is often concentrated in close vicinity to the transducer tip, while the bulk of the processed material may not be subjected to sufficiently high ultrasound intensity [32]. In addition to poor product treatment, the high acoustic intensity near the horn tip can also lead to pronounced erosion of the sonotrode material through violent cavitation bubble collapse in close proximity [40]. For that reason, computational models have been sought to help characterising and optimising the performance of such reactors and to facilitate scaling up.

Klima et al. [23] developed a 3D model of a cylindrical low-frequency ultrasound reactor with an ultrasound horn (also referred to transducer or sonotrode) inserted from the top (Fig. 12a) in COMSOL Multiphysics and used this to predict the acoustic intensity distribution by solving the linear wave equation. Their model did not include generation of flow or increase in temperature through sound dissipation, or the formation of cavitation bubbles that strongly attenuate the sound transmission due to scattering, all of which affect the acoustic pressure/intensity distribution. However, they were able to qualitatively validate the model predictions by comparing the intensity distribution to photographs of induced cavitation clouds (Fig. 12b). They showed that the intensity distribution is strongly dependent on the location of the sonotrode in the reactor and that appropriate insertion depth shifted the acoustic intensity from the sonotrode tip into the bulk of the sonoreactor (Fig. 13). They have explained this by the occurrence of multiple reflections and the behaviour of the reactor as a resonator; therefore, the optimum location of the ultrasound horn is strongly dependent on the size of the reactor, its geometrical configuration, as well as the product treated.

Other groups have focused on modelling the hydro- and thermodynamic behaviour of low-frequency sonoreactors, still neglecting the cavitational effects. For instance, Trujillo and Knoerzer [56] reported on the development of a Multiphysics model capable of simulating the formation of a jet-like acoustic streaming generated by a sonotrode placed in water in a low-frequency (20 kHz) high-power ultrasound reactor. The acoustic power was assumed to be dissipated within close proximity to the horn, and the acoustic energy was completely converted into kinetic and thermal energy leading to a jet being formed and directed away from the sonotrode, while the temperature was increasing in the bulk of the treated fluid. The model was validated by utilising published data from Kumar et al. [33] where fluid movement was measured by laser Doppler anemometry.

Figure 14 shows the computational representation of the system investigated by Kumar et al. [33] and Trujillo and Knoerzer [56] in 3D and 2D. Full 3D and axis-symmetric 2D models predicted almost identical values; therefore, the fact that the computational demand of the 3D model was very high, all further models for comparison with the LDA data were solved in 2D only. Figure 15 shows a qualitative comparison of the velocity profile predicted by the model and the one measured by LDA for a specific power input. Both prediction and measurement show the jet being formed just underneath the horn tip with much lower velocities throughout the rest of the reactor.

Apart from visual comparisons, the authors also performed a quantitative validation of the model by comparing the predicted values of the axial velocity at a number of heights and radii (Fig. 16) and found good agreement.

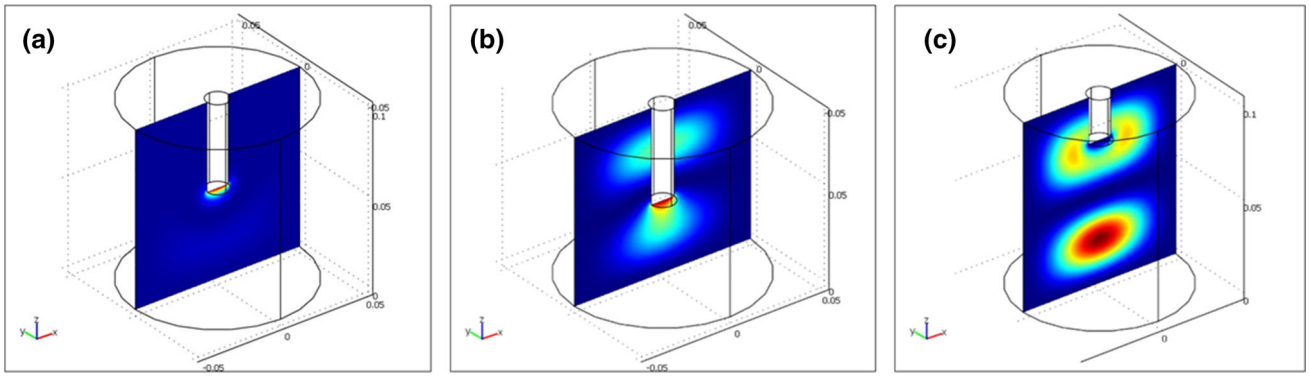

Fig. 13 **a** Sonotrode inserted by half the height of the reactor showing highest acoustic intensity at the horn tip; **b** sonotrode inserted by approximately 66 % of the reactor height showing improvement of acoustic intensity distribution; **c** sonotrode inserted by approximately 25 % of the reactor height showing a shift of high-intensity zones away from the sonotrode tip (adapted from Klima et al. [23]; for colour representation, the reader is referred to the online version of this article)

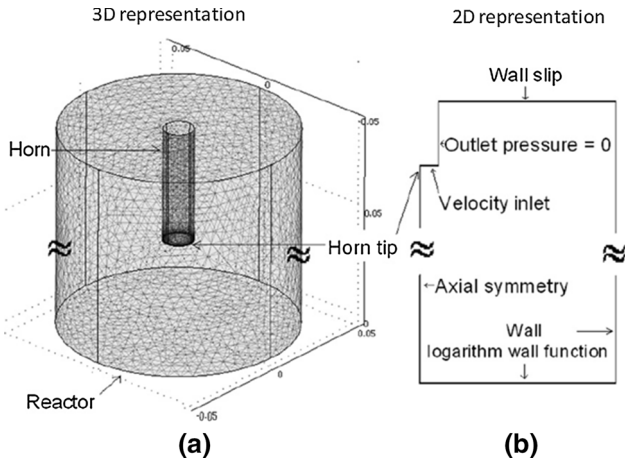

Fig. 14 Depiction of the geometry of the investigated system; **a** 3D representation and **b** 2D axis-symmetric representation, including the boundary conditions of the model (from Trujillo and Knoerzer [56]

Similar modelling approaches were recently published by Schenker et al. [52] and Parvizian et al. [47] for low- and high-frequency applications, respectively.

Schenker et al. [52] utilised particle imaging velocimetry (PIV) for experimental validation of the jet formation in a low-frequency ultrasound reactor. While from a numerical modelling perspective, the findings were similar to those of Trujillo and Knoerzer [56] and their postprocessing evaluations include estimations on the treatment time required for the entire volume (in their case, 200 particles suspended in the liquid) to pass through the zone of high acoustic intensity (cavitation zone). This is a helpful tool in designing the process in terms of required residence time for any given product, reactor geometry and other process conditions.

Parvizian et al. [47] modelled the flow characteristics and micromixing efficiency in a tubular, continuously operating high-frequency (1.7 MHz) reactor (Fig. 17a). The reported chemical application is not directly related to food processing; however, applications in the food space of such reactors could include modulations of enzymatic reaction, enhanced mass transfer in extraction and separation processes, inducing stress responses in living tissues for texture modification among others.

They report on the development of a 3D model (Fig. 17b) in FLUENT 6.2 (Ansys Inc., Canonsburg, PA, USA), in which generic fluid dynamics was coupled with further induced micromixing by including the vibrations of the high-frequency piezoceramic transducers and the high-frequency wave propagation, as well as the kinetics for the Villermaux/Dushman reaction, widely used for evaluating micromixing efficiency. They found that the flow patterns changed significantly after switching on two and four transducers, compared to the flow that is observed without the presence of ultrasound, leading to a more efficient reaction, i.e. more efficient micromixing (Fig. 18). The authors conclude that this model enables the determination of optimum number and locations of ultrasound transducers to achieve maximum micromixing in any given reactor geometry.

Although not specifically used for food processing, the studies published by Jamshidi et al. [16] are still relevant within the scope of this review as they describe the modelling of sound intensity and the interactions of acoustic field and cavitation.

Jamshidi et al. [16] reported on numerical modelling approaches to investigate the impact of different chamber (reactor) configurations and process parameters on the sound intensity in the reactor. The 3D models (Fig. 19a) of two different configurations were developed in COMSOL Multiphysics and different frequencies and power levels evaluated.

The models were useful in predicting cavitation zones, and the authors concluded that optimisation of both

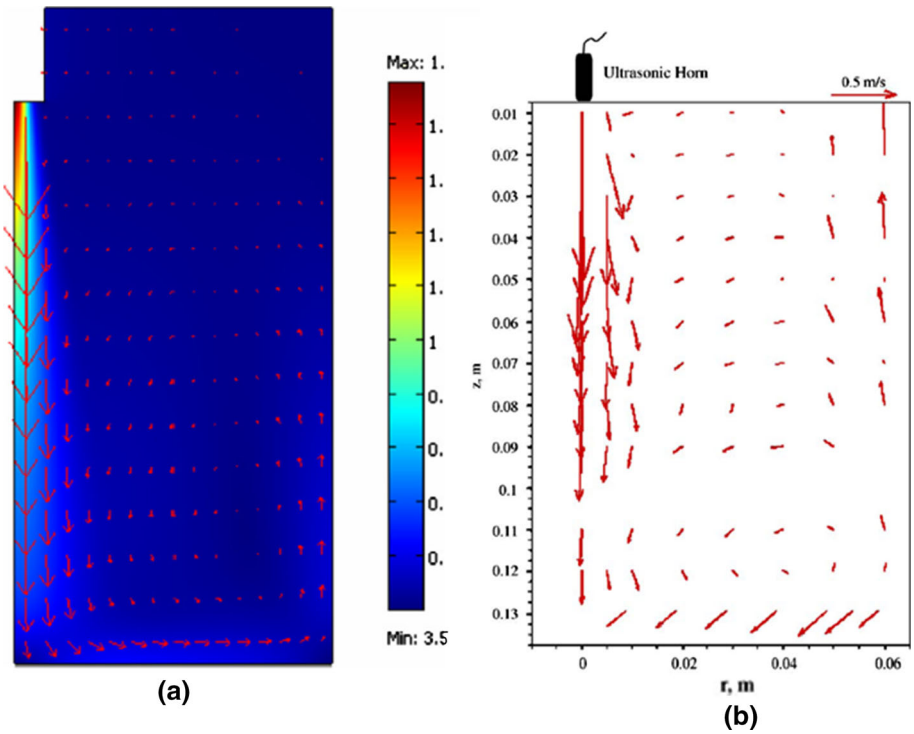

Fig. 15 Visual comparison of the predicted (**a**) and measured by LDA (**b**) flow profiles in the investigated system at a specific power input of 35 kW/m^3 (from Trujillo and Knoerzer [56]; for colour representation, the reader is referred to the online version of this article)

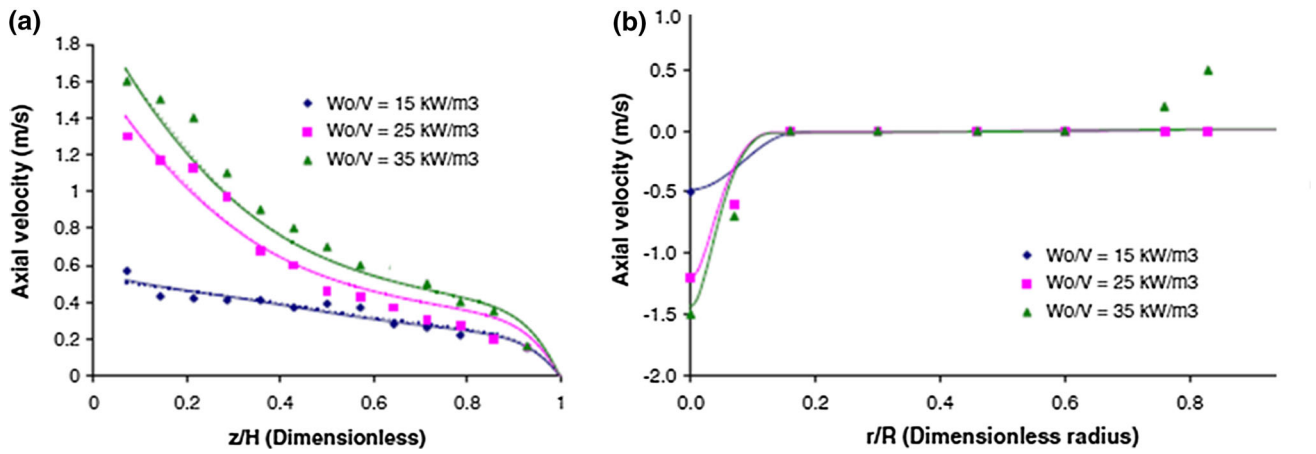

Fig. 16 Quantitative comparison of model predictions and experimentally determined values of **a** the axial velocity at different height levels under the horn tip and **b** different radii at height level of 13 % of the total reactor height (from Trujillo and Knoerzer [56])

frequency and power level is possible with respect to location, distribution and intensity of cavitation (Fig. 19b–d). While the reactor presented in this study is used for the production of nanoparticles, this modelling approach is very useful also in food processing, e.g. in emulsification or extraction processes, where high-intensity ultrasound can be used for breakage of droplets or cells. However, the study was based on a number of assumptions with respect to the cavitation formation, which can lead to inaccurate predictions in some cases. Therefore, Jamshidi and Brenner [15] have reported on a more fundamental study, where the motion of individual bubbles in the bubble cloud under the action of acoustic pressure is investigated numerically including bubble radial dynamics. These 2D models (Fig. 20a) were developed in OpenFOAM, and the results clearly show that the motion of the bubbles and the structure of the cavitation cloud are predicted accurately, as can be seen in Fig. 20b, which shows the conical structure of the cavitation bubbles in the vicinity of an ultrasound horn.

Apart from low-frequency ultrasound applications, high-frequency ultrasound has been studied mainly with respect

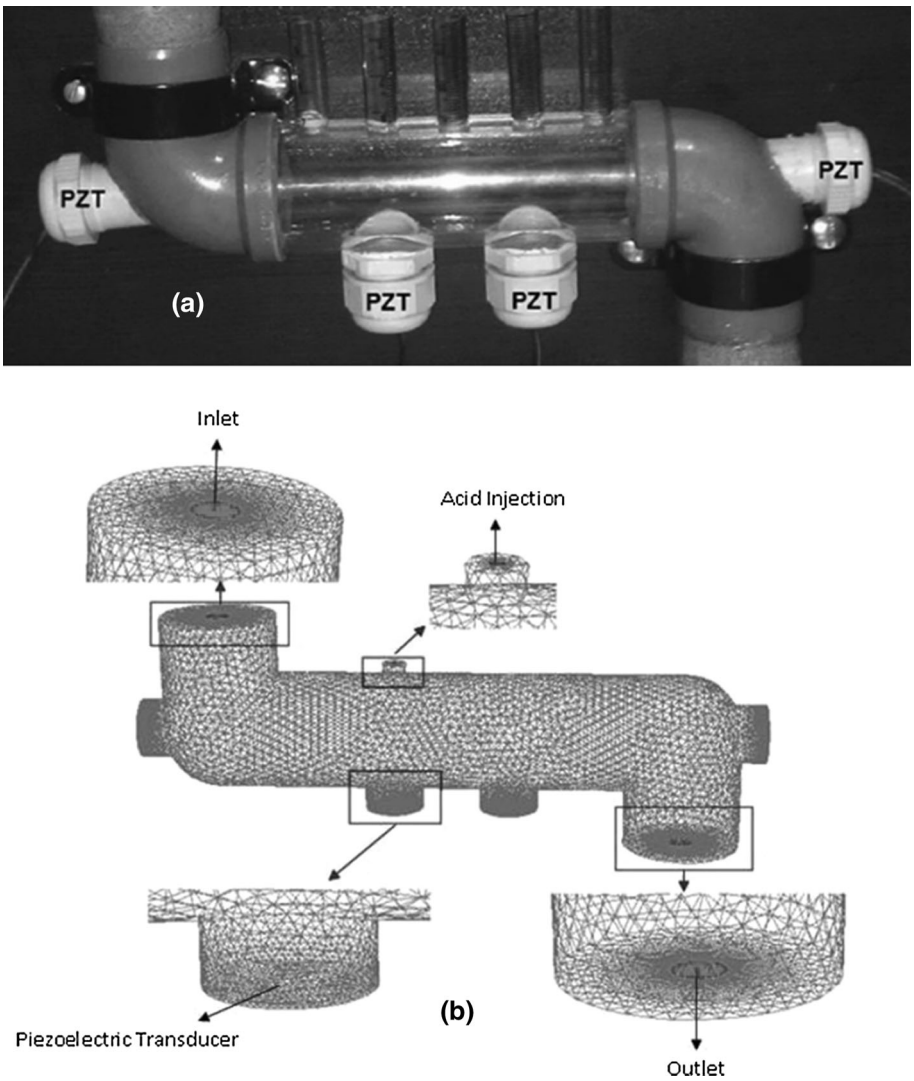

Fig. 17 **a** Experimental set-up of the tubular, continuous flow ultrasound reactor (*PZT* piezoelectric transducer); **b** computational model of the ultrasound reactor (adapted from Parvizian et al. [47]

to separation techniques to trap or fractionate suspended particles or droplets from a bulk-phase liquid [18–20, 36–38] by means of ultrasonic standing waves (USW). An extensive review on the basics and applications of modelling megasonics for particle separation was recently done by Trujillo et al. [55]. The only study on modelling megasonics relevant to food processing at a scale greater than a few millimetres was reported by Trujillo et al. [54].

Most of the models found in the literature are applied for microfluidic devices. Those devices use continuous laminar flow for separation of particles [35]. Microfluidic devices usually utilise half-wavelength resonators with a pressure node located at the centre of the flow channel while antinodes are located at the channel walls. For larger multimodal applications, Trujillo et al. [54] published on the development of a Multiphysics model for a high-frequency ultrasound application for separation of particles out of a continuous water phase. The simulated separation reactor is shown in Fig. 21a. The model included solving for the mechanical displacement of the reactor walls, leading to the formation of an acoustic pressure field (indicated in Fig. 21a for a fixed frequency of 1.54 MHz as a thin band in the reactor and a magnified view in Fig. 21b, p), followed by predicting the acoustic radiation force acting on suspended particles (Fig. 21b, F_{Rad}). Finally, this (transient) force was utilised to solve for the movement of the particle phase to the nodes of the ultrasonic standing wave (Fig. 21b, X_{P}) and frequency ramping, leading to active separation of the particles away from the transducer plate towards the reflector. The model accounts for changes in the concentration of particles by modifying the mass transport equation so that it includes the effect of the acoustic field to alter the concentration of particles. The authors report that the model is more suitable for larger scale applications where more pronounced gradients on the acoustic field and particle concentration profile are present.

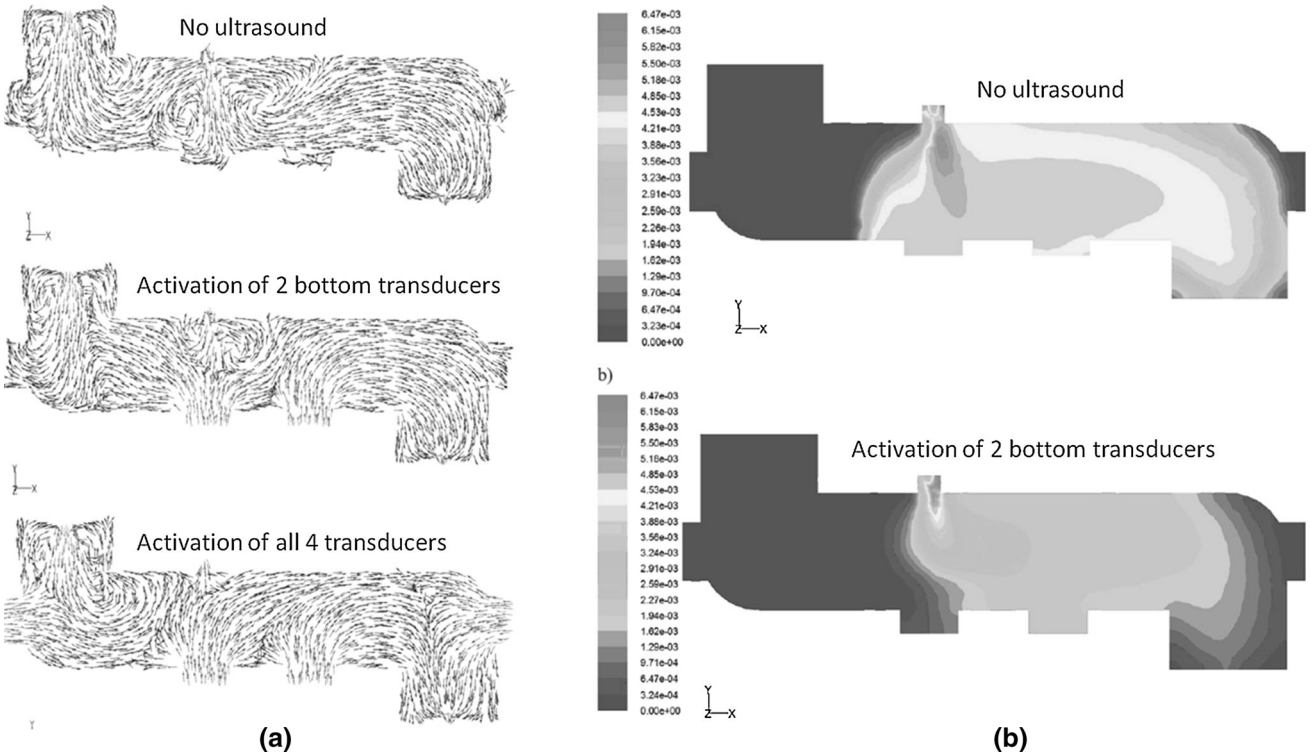

Fig. 18 **a** Flow patterns in the tubular reactor without ultrasound and after switching on two and four transducers, respectively; **b** contour plots of I_3^- (end product of chemical reaction) mass fraction yields without ultrasound and after switching on two bottom transducers, indicating greater reaction yield with ultrasound exposure (adapted from Parvizian et al. [47]

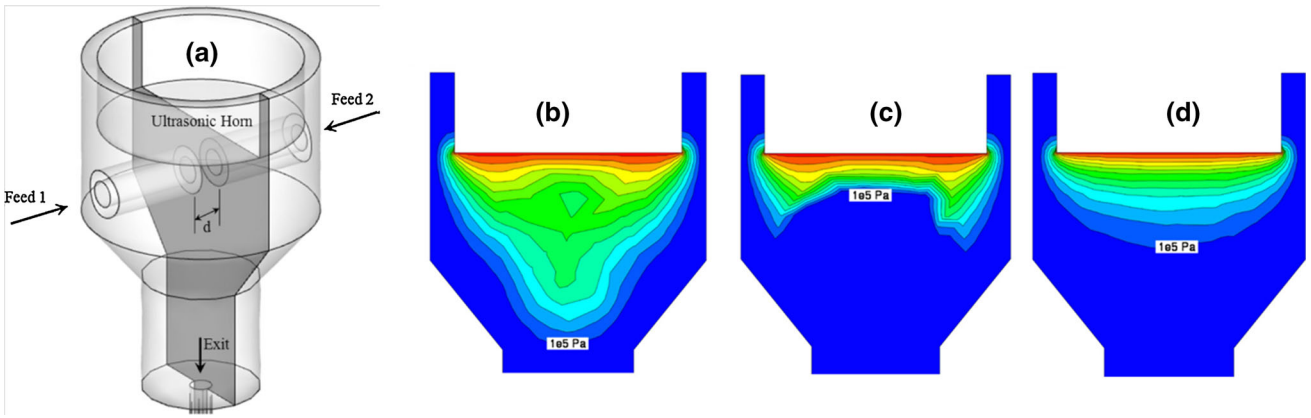

Fig. 19 **a** Schematic representation of the reactor; d is the parameter changed for the different configurations; solid cross section shows the plane used in the 2D plots (**b**, **c**, **d**); predicted cavitation distribution at a frequency of **a** 10, **b** 20 and **c** 30 kHz. A frequency of 10 kHz produced a preferable cavitation distribution for this particular configuration (adapted from Jamshidi et al. [16]; for colour representation, the reader is referred to the online version of this article)

They then compared digitised images of the actual process at discrete times of 0, 40 and 120 s (Fig. 22a) with the predicted particle band formation and transient band movement. As shown in Fig. 22b at a discrete time of 120 s, measurement and predictions agreed well. Figure 22c shows a parity plot of the measured and predicted band locations for all three time steps; as can be seen, a very good agreement was found.

Outlook

It is widely established that innovative technologies are the means to meet a need and capture an opportunity, particularly around the manufacture of attractive, new, high-quality food products with fresh-like quality attributes, ensured safety and shelf life, and more sustainable manufacturing. The main incentive for applying these new

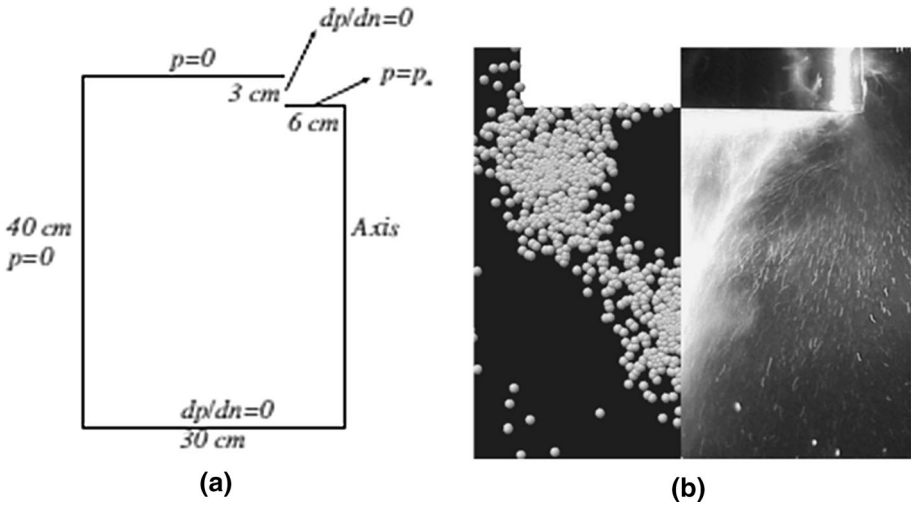

Fig. 20 **a** Geometry of 2D model including relevant boundary conditions; **b** predicted and experimentally determined cavitation bubble distribution (adapted from Jamshidi and Brenner [15])

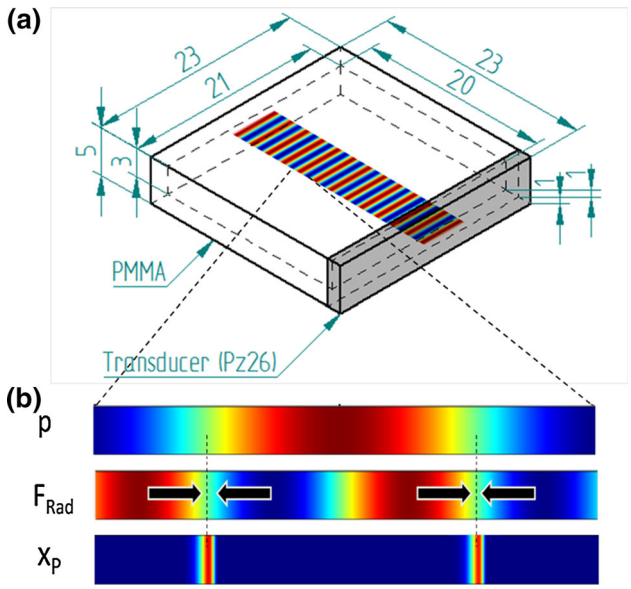

Fig. 21 **a** Schematic representation of the investigated treatment chamber with pressure distribution for a fixed frequency of 1.54 MHz, and magnification of one wavelength of the pressure distribution (**b**; p), the resulting acoustic force (**b**; F_{Rad}) and the particles concentrated at the nodes of the pressure wave at the fixed frequency (**b**; X_{P}) (adapted from Trujillo et al. [54]; for colour representation, the reader is referred to the online version of this article)

technologies should focus on inducing disruptive innovation in the food manufacturing industry rather than solely providing incremental improvements of existing processes.

Validated Multiphysics models have been used to characterise, evaluate and optimise existing equipment for innovative food processing technologies, and such modelling strategies will be able to assist in further developing these technologies for effective and efficient implementation in the food manufacturing industry. Without such modelling capabilities, relying on the traditional approach of trial and error, the development will be slow, and in some instances, a sufficient performance justifying utilisation in industry may never happen. Future trends may include, but are not limited to, more extensive coupling of predictive models for microbial, chemical and biochemical reactions with the predictions of the CFD models for various technologies and purposes and utilising these coupled models for process and equipment improvement and optimisation; models at various scales (multi-scale covering micro- to macro-scale) may provide further insights and benefits, as well as models that include, e.g. corrosion or erosion effects, which will then be useful to predict wear and tear of the equipment, give an estimation on when certain parts need to be replaced, and allow for process modification to reduce equipment deterioration.

To date, model validation was mainly done through measurement of a limited number of process variables, such as temperature or in some cases flow distribution, and then comparison with the model prediction. When this validation has proven successful, other process variables that cannot be easily measured, for example, electric field distribution in PEF processes, were then assumed to also be accurately predicted. In future studies, it would be beneficial to explore and eventually utilise measurement techniques that allow for the quantification of other important and technology-specific process variables, such as electric or electromagnetic field distribution. Furthermore, more direct and quantitative validation of predicted process outcomes (e.g. bacterial spore inactivation, chemical reaction products, degradation of quality attributes such as colour and/or texture) will help to improve reliability of the models and utilisation of Multiphysics modelling in the food industry.

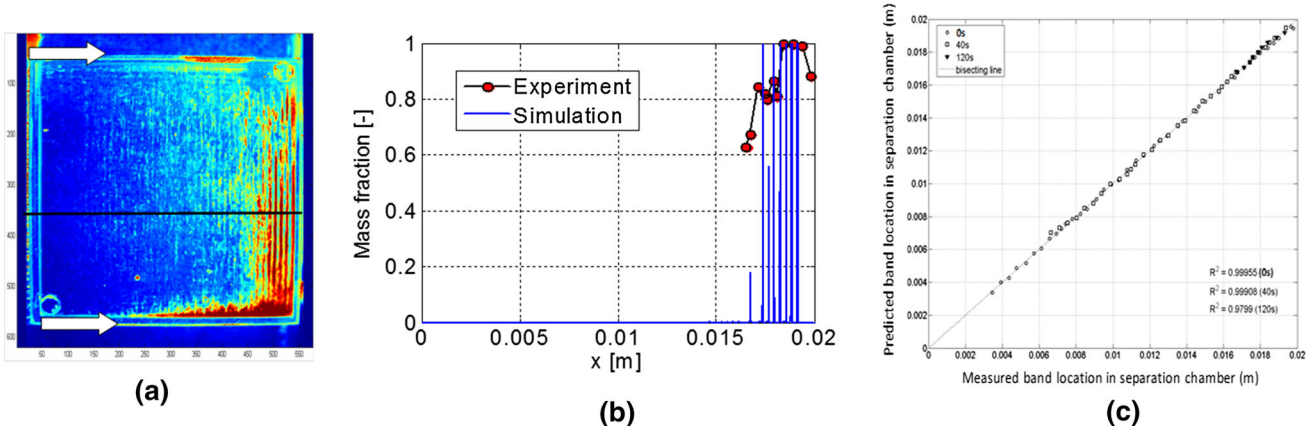

Fig. 22 **a** Digitised image of actual process at a discrete time of 120 s (false colour representation; the *black line* indicating the area for comparison with the model prediction); **b** comparison of the mass fraction of the separated particles measured and predicted; **c** parity plot of the measured and predicted band locations at discrete time steps of 0, 40 and 120 s (adapted from Trujillo et al. [54]; for colour representation, the reader is referred to the online version of this article)

References

1. Barbosa-Canovas GV, Albaali A, Juliano P, Knoerzer K (2011) Introduction to innovative food processing technologies: background, advantages, issues, and need for multiphysics modeling. In: Knoerzer K, Juliano P, Roupas P, Versteeg C (eds) Innovative food processing technologies: advances in multiphysics simulation. Wiley Blackwell, Ames, pp 3–22
2. Beck SM, Sabarez H, Gaukel V, Knoerzer K (2014) Enhancement of convective drying by application of airborne ultrasound—a response surface approach. Ultrason Sonochem (in press)
3. Buckow R, Baumann P, Schroeder S, Knoerzer K (2011) Effect of dimensions and geometry of co-field and co-linear pulsed electric field treatment chambers on electric field strength and energy utilisation. J Food Eng 105(3):545–556
4. Buckow R, Ng S, Toepfl S (2013) Pulsed electric field processing of orange juice: a review on microbial, enzymatic, nutritional, and sensory quality and stability. Compr Rev Food Sci Food Saf 12(5):455–467
5. Buckow R, Schroeder S, Berres P, Baumann P, Knoerzer K (2010) Simulation and evaluation of pilot-scale pulsed electric field (PEF) processing. J Food Eng 101(1):67–77
6. Buckow R, Semrau J, Sui Q, Wan J, Knoerzer K (2012) Numerical evaluation of lactoperoxidase inactivation during continuous pulsed electric field processing. Biotechnol Prog 28(5):1363–1375
7. Day L, Xu M, Oiseth SK, Mawson R (2012) Improved mechanical properties of retorted carrots by ultrasonic pre-treatments. Ultrason Sonochem 19(3):427–434
8. Delgado A, Rauh C, Kowalczyk W, Baars A (2008) Review of modelling and simulation of high pressure treatment of materials of biological origin. Trends Food Sci Technol 19(6):329–336
9. Fiala A, Wouters P, van den Bosch E, Creyghton Y (2001) Coupled electrical-fluid model of pulsed electric field treatment in a model food system. Innov Food Sci Emerg Technol 2(4):229–238
10. Gerlach D, Alleborn N, Baars A, Delgado A, Moritz J, Knorr D (2008) Numerical simulations of pulsed electric fields for food preservation: a review. Innov Food Sci Emerg Technol 9(4):408–417
11. Ghani AGA, Farid MM (2007) Numerical simulation of solid–liquid food mixture in a high pressure processing unit using computational fluid dynamics. J Food Eng 80(4):1031–1042
12. Gogate PR, Kabadi AM (2009) A review of applications of cavitation in biochemical engineering/biotechnology. Biochem Eng J 44(1):60–72
13. Grauwet T, Rauh C, Van der Plancken I, Vervoort L, Hendrickx M, Delgado A, Van Loey A (2012) Potential and limitations of methods for temperature uniformity mapping in high pressure thermal processing. Trends Food Sci Technol 23(2):97–110
14. Jaeger H, Meneses N, Knorr D (2009) Impact of PEF treatment inhomogeneity such as electric field distribution, flow characteristics and temperature effects on the inactivation of *E. coli* and milk alkaline phosphatase. Innov Food Sci Emerg Technol 10(4):470–480
15. Jamshidi R, Brenner G (2014) An Euler–Lagrange method considering bubble radial dynamics for modeling sonochemical reactors. Ultrason Sonochem 21(1):154–161
16. Jamshidi R, Pohl B, Peuker UA, Brenner G (2012) Numerical investigation of sonochemical reactors considering the effect of inhomogeneous bubble clouds on ultrasonic wave propagation. Chem Eng J 189:364–375
17. Juliano P, Knoerzer K, Fryer P, Versteeg C (2009) *C. botulinum* inactivation kinetics implemented in a computational model of a high pressure sterilization process. Biotechnol Prog 25(1):163–175
18. Juliano P, Swiergon P, Lee KH, Gee PT, Clarke PT, Augustin MA (2013) Effects of pilot plant-scale ultrasound on palm oil separation and oil quality. J Am Oil Chem Soc 90(8):1253–1260
19. Juliano P, Swiergon P, Mawson R, Knoerzer K, Augustin MA (2013) Application of ultrasound for oil separation and recovery of palm oil. J Am Oil Chem Soc 90(4):579–588
20. Juliano P, Temmel S, Rout M, Swiergon P, Mawson R, Knoerzer K (2013) Creaming enhancement in a liter scale ultrasonic reactor at selected transducer configurations and frequencies. Ultrason Sonochem 20:52–62
21. Kang H, Lin Y, Ling G, Jianping W (2013) Coupled simulations in colinear and coaxial continuous pulsed electric field treatment chambers. Trans ASABE 56(4):1473–1484
22. Khurana M, Karwe MV (2009) Numerical prediction of temperature distribution and measurement of temperature in a high

hydrostatic pressure food processor. Food Bioprocess Technol 2(3):279–290
23. Klima J, Frias-Ferrer A, Gonzalez-Garcia J, Ludvik J, Saez V, Iniesta J (2007) Optimisation of 20 kHz sonoreactor geometry on the basis of numerical simulation of local ultrasonic intensity and qualitative comparison with experimental results. Ultrason Sonochem 14(1):19–28
24. Knoerzer K, Buckow R, Juliano P, Chapman B, Versteeg C (2010) Carrier optimisation in a pilot-scale high pressure sterilisation plant—an iterative CFD approach. J Food Eng 97(2):199–207
25. Knoerzer K, Buckow R, Sanguansri P, Versteeg C (2010) Adiabatic compression heating coefficients for high-pressure processing of water, propylene-glycol and mixtures—a combined experimental and numerical approach. J Food Eng 96(2):229–238
26. Knoerzer K, Buckow R, Versteeg C (2010) Adiabatic compression heating coefficients for high pressure processing—a study of some insulating polymer materials. J Food Eng 98(1):110–119
27. Knoerzer K, Chapman B (2011) Effect of material properties and processing conditions on the prediction accuracy of a CFD model for simulating high pressure thermal (HPT) processing. J Food Eng 104(3):404–413
28. Knoerzer K, Juliano P, Gladman S, Versteeg C, Fryer P (2007) A computational model for temperature and sterility distributions in a pilot-scale high-pressure high-temperature process. AIChE J 53(11):2996–3010
29. Knoerzer K, Juliano P, Roupas P, Versteeg C (2011) Innovative food processing technologies: advances in Multiphysics simulation. Wiley Blackwell, Ames
30. Knoerzer K, ZArnold M, Buckow R (2011) Utilising Multiphysics modelling to predict microbial inactivation induced by pulsed electric field processing. In: ICEF11—11th international congress on engineering and food, Athens, Greece, 22–26 May 2011
31. Knoerzer K, Baumann P, Buckow R (2012) An iterative modelling approach for improving the performance of a pulsed electric field (PEF) treatment chamber. Comput Chem Eng 37:48–63
32. Kumar A, Gogate PR, Pandit AB (2007) Mapping the efficacy of new designs for large scale sonochemical reactors. Ultrason Sonochem 14(5):538–544
33. Kumar A, Kumaresan T, Pandit AB, Joshi JB (2006) Characterization of flow phenomena induced by ultrasonic horn. Chem Eng Sci 61(22):7410–7420
34. Kumar SS, Balasubrahmanyam A, Sundar PS, Gogate PR, Deshpande VD, Shukla SR, Pandit AB (2009) Characterization of sonochemical reactor for physicochemical transformations. Ind Eng Chem Res 48(21):9402–9407
35. Lenshof A, Magnusson C, Laurell T (2012) Acoustofluidics 8: applications of acoustophoresis in continuous flow microsystems. Lab Chip 12(7):1210–1223
36. Leong T, Johansson L, Juliano P, Mawson R, McArthur S, Manasseh R (2014) Design parameters for the separation of fat from raw milk in an ultrasonic litre-scale vessel. Ultrason Sonochem 21(4):1289–1298
37. Leong T, Johansson L, Juliano P, McArthur SL, Manasseh R (2013) Ultrasonic separation of particulate fluids in small and large scale systems: a review. Ind Eng Chem Res 52(47):16555–16576
38. Leong T, Juliano P, Johansson L, Mawson R, McArthur S, Manasseh R (2014) Temperature effects on the ultrasonic separation of fat from natural whole milk. Ultrason Sonochem 21(6):2092–2098
39. Lindgren M, Aronsson K, Galt S, Ohlsson T (2002) Simulation of the temperature increase in pulsed electric field (PEF) continuous flow treatment chambers. Innov Food Sci Emerg Technol 3(3):233–245
40. Mawson R, Rout M, Swiergon P, Ripoll Munho G, Singh T, Knoerzer K, Juliano P (2014) Production of particulates from transducer erosion: implications on food safety. Ultrason Sonochem 21(6):2122–2130
41. Meneses N, Jaeger H, Knorr D (2011) Minimization of thermal impact by application of electrode cooling in a co-linear PEF treatment chamber. J Food Sci 76(8):E536–E543
42. Meneses N, Jaeger H, Knorr D (2011) pH-changes during pulsed electric field treatments—numerical simulation and in situ impact on polyphenoloxidase inactivation. Innov Food Sci Emerg Technol 12(4):499–504
43. Meneses N, Jaeger H, Moritz J, Knorr D (2011) Impact of insulator shape, flow rate and electrical parameters on inactivation of *E. coli* using a continuous co-linear PEF system. Innov Food Sci Emerg Technol 12(1):6–12
44. Mujica-Paz H, Valdez-Fragoso A, Samson CT, Welti-Chanes J, Torres JA (2011) High-pressure processing technologies for the pasteurization and sterilization of foods. Food Bioprocess Technol 4(6):969–985
45. Oey I, Lille M, Loey A, Hendrickx M (2008) Effect of high-pressure processing on colour, texture and flavour of fruit- and vegetable-based food products: a review. Trends Food Sci Technol 19(6):320–328
46. Olivier S, Bull M, Stone G, Diepenbeek R, Kormelink F, Jacops L, Chapman B (2011) Strong and consistently synergistic inactivation of spores of spoilage-associated *Bacillus* and *Geobacillus* spp. by high pressure and heat compared with inactivation by heat alone. Appl Environ Microbiol 77(7):2317–2324
47. Parvizian F, Rahimi M, Azimi N, Alsairafi AA (2014) CFD modeling of micromixing and velocity distribution in a 1.7-MHz tubular sonoreactor. Chem Eng Technol 37(1):113–122
48. Rauh C, Baars A, Delgado A (2009) Uniformity of enzyme inactivation in a short-time high-pressure process. J Food Eng 91(1):154–163
49. Rodriguez G, Riera E, Gallego-Juarez JA, Acosta VM, Pinto A, Martinez I, Blanco A (2010) Experimental study of defoaming by air-borne power ultrasonic technology. International congress on ultrasonics physics procedia, vol 1, pp 135–139
50. Sabarez H, Gallego-Juarez J, Riera E (2012) Ultrasonic-assisted convective drying of apple slices. Drying Technol 30(9):989–997
51. Saldana G, Puertolas E, Alvarez I, Meneses N, Knorr D, Raso J (2010) Evaluation of a static treatment chamber to investigate kinetics of microbial inactivation by pulsed electric fields at different temperatures at quasi-isothermal conditions. J Food Eng 100(2):349–356
52. Schenker MC, Pourquie MJBM, Eskin DG, Boersma BJ (2013) PIV quantification of the flow induced by an ultrasonic horn and numerical modeling of the flow and related processing times. Ultrason Sonochem 20(1):502–509
53. Smith NAS, Knoerzer K, Ramos AM (2014) Evaluation of the differences of process variables in vertical and horizontal configurations of high pressure thermal (HPT) processing systems through numerical modelling. Innov Food Sci Emerg Technol 22:51–62
54. Trujillo FJ, Eberhardt S, Moeller D, Dual J, Knoerzer K (2013) Multiphysics modelling of the separation of suspended particles via frequency ramping of ultrasonic standing waves. Ultrason Sonochem 20(2):655–666
55. Trujillo FJ, Juliano P, Barbosa-Canovas G, Knoerzer K (2014) Separation of suspensions and emulsions via ultrasonic standing waves—a review. Ultrason Sonochem 21(6):2151–2164
56. Trujillo FJ, Knoerzer K (2011) A computational modeling approach of the jet-like acoustic streaming and heat generation induced by low frequency high power ultrasonic horn reactors. Ultrason Sonochem 18(6):1263–1273